

# Effect of a blade shape on hydraulic and mechanical properties of a single - blade impeller

Matej Kurilla<sup>1,\*</sup>, Branislav Knížat<sup>1</sup>, Zoltán Csuka<sup>1</sup>, and Maroš Hyriak<sup>2</sup>

<sup>1</sup>Slovak University of Technology in Bratislava, Nám. slobody 17, 812 31 Bratislava, Slovakia

<sup>2</sup>PRAKTIK PUMP, Jesenského 63, 96001 Zvolen, Slovakia

**Abstract.** Single-blade centrifugal pumps with a screw-shaped blade are perspective hydraulic machines with possible usage in many areas. According to the non-symmetrical impeller shape, mechanical properties, resulting from a dynamic balancing, are not fulfilled automatically. The way of designing of an impeller which enables fulfilled main requests such as good hydraulic, mechanical properties and the ball passage diameter, is described in this academic paper.

## 1 Introduction

Centrifugal pumps with a single-blade impeller represent an important segment of the hydraulic machines in the wastewater pumping area. The advantages include a large passed solids size and good cavitation properties by remaining a relatively high efficiency in the wide flowrate range [4]. The construction is generally simple and massive, so single-blade centrifugal pumps are characterized by long lifetime and high reliability during the running process. Solids with diameter equal to the diameter of the suction pipe are able to pass through the impeller without any damage. That's why this type of pumps is used in food processing for pumping fruits, fish, etc. Many types of single-blade centrifugal pumps can be recognized, differing mainly in the blade shape. This paper is devoted to hydrodynamic pumps with the screw-shaped blade.

## 2 Flow in a single-blade impeller

Flow in a single-blade impeller has got its own specific features that differentiate this pump from other conventional centrifugal pumps with multi-blade impellers. In respect of a long wrap angle, the blade outlet angle accomplishes relatively low values. As a result, the Q-Y curves are considerably steep and also linear, resulting in the stability in the pump operation. Due to the single blade, the impeller is geometrically asymmetric with respect to the rotational axis. The same applies to a diffuser which is the volute casing.

Rotational, asymmetrical pressure and velocity fields interact with also non-symmetrical fluxional field in the stator. Accordingly, non-zero radial thrust acts on an impeller, even in

---

\* Corresponding author: [matej.kurilla@stuba.sk](mailto:matej.kurilla@stuba.sk)

the design point. The radial thrust increases along with a higher blade outlet angle and also with higher flowrates [5]. The result is that the radial force problem is much stronger than with conventional centrifugal pumps. Considerable researcher's effort is focused on the knowledge of energy transformation mechanism in single-blade pumps. The aim is decreasing of losses and therefore raising the efficiency. According to the fluxional fields asymmetry it is possible to observe the substantial fluctuation of performance parameters in the pump during one revolution. Performance parameters are torque, specific energy, flowrate, and shaft power.

A designing process uses standard design methods [2] which don't provide as accurate methodology as necessary. Consequently, these methods are combined with CFD computation methods [3]. We consider a shape of the dimensionless function of specific energy, in the design process - equation (1):

$$\Psi = \Psi_t - \Theta(\Phi_2) \quad (1)$$

The dimensionless flowrate  $\Phi_2$  and theoretical specific energy  $\Psi_t$  are given by the following equations [7]:

$$\Phi_2 = \frac{Q}{\eta_V A_2 U_2} \quad (2)$$

$$\Psi_t = \sigma_Y - \frac{\Phi_2}{\tan \beta_2} \quad (3)$$

In equations (1) to (3) is  $\Psi_t$  – theoretical specific energy,  $\beta_2$  – blade outlet angle,  $\eta_V$  – volume efficiency,  $A_2$  – outlet area a  $U_2$  – tangential outlet velocity.

The curve  $\Psi$ - $\Phi_2$ , respectively  $Y$ - $Q$  (specific energy - flowrate) is shaped by the  $\sigma_Y$  and  $\Theta(\Phi_2)$  parameter, i.e., the slip factor [7] and the hydraulic losses function.

The slip factor of the flow in the impeller  $\sigma_Y$ , in the equation (3), is about 0,4 for single-blade impellers. It characterizes imperfect guidance of a liquid [6]. We can estimate hydraulic losses in the optimal point, based on supposed efficiency of the pump.

A subject of the proposal is meridional cut of the pump as well as a shape of the blade. Considerably important fact needs to be considered here, in contrast with conventional centrifugal pumps. Owing to the asymmetric blade shape, the computed blade designed to fulfil energetic parameters, causes dynamic unbalance of the whole rotational part of the pump. The impeller loses its mechanical properties as a rotor. Accordingly, the impeller has to be balanced by adding of additional material. It influences retroactively the shape of the blade channel and the whole hydraulic solution. We will refer to influence of the dynamic balancing of the impeller on hydraulic parameters of the pump in this paper.

## 2.1 Hydraulic parameters of the pump

Mechanical and hydraulic properties of the impeller were researched on a single-blade spiral pump with parameters in the Table 1. For these parameters a pump with two impeller alternatives has been designed, hereinafter referred as A and B. Both impellers have the same base what does concern geometrical parameters. They differ from each other in the level of balance when the impeller A is unbalanced and the impeller B is dynamically balanced. A diameter of the suction, as well as discharge pipe of the pump, was 50 mm. Single-blade pumps with such hydraulic parameters have an expected efficiency approximately in the interval between 50 % and 60 %. All of the results are given for clean

water. Internal spaces of the pump from suction to discharge, including the impeller and the spiral casing were designed so a ball with the diameter of 50 mm passes through the pump.

**Table 1.** Hydraulic parameters of the pump.

Parameter	Value	Description
Q [m <sup>3</sup> /s]	0.011	Flowrate
Y [J/kg]	105	Specific energy
n [s <sup>-1</sup> ]	2 900	Speed
n <sub>b</sub> [-]	0.15	Specific speed

The spiral casing were made of welded metal plates.

### 2.2 Geometric parameters of impellers

Two impellers marked as A and B were made to test their mechanical and hydraulic properties. Both impellers have the same meridional cut and the suction side of blades is the same expandable line surface. They are manufactured as semi-open impellers. The impeller A is dynamically and statically unbalanced. Mechanical properties of this impeller are substantially adverse. However, the hydraulic properties are considerably good because the blade channel shape directly responses to the calculation. The basic blade shape is illustrated in the Figure 1. The red point C represents the location of the center of gravity of the impeller A. In the design, the basic course of the blade and its mass distribution is chosen, so the center of the gravity lies as close as possible to the rotational axis. This is achieved by the inclination of cut lines A-B, i.e. by the angle  $\vartheta$ , exactly like the Figure 1 shows. The curves *a* and *b* represent then streamlines on the front respectively back plate. It isn't possible to totally balance the impeller only with the blade shaping. The impeller has to be dynamically balanced by adding of material.

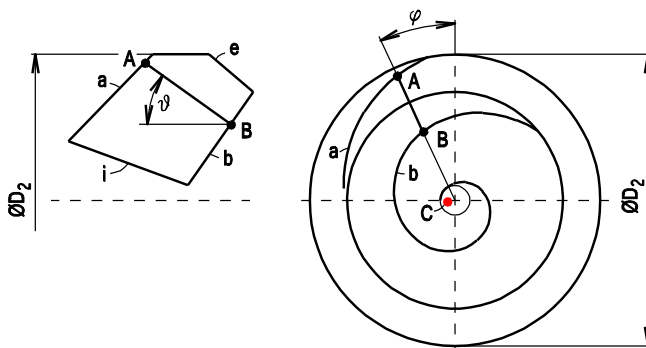


**Fig. 1.** The impeller blade as a ruled surface.

The geometrical parameters of both impellers are shown in the Table 2. The impeller's photo is in the Figure 2. The impeller A was made by welding of a steel plate (the blade) and the impeller B was drawn in a CAD programme and printed on a 3D printer from ABS plastic.

**Table 2.** Geometry parameters of impellers.

	<b>Impeller A</b>	<b>Impeller B</b>	<b>Description</b>
$D_1$ [mm]	50		Inlet diameter
$D_2$ [mm]	138		Outlet diameter
$\beta_2$ [°]	8.2		Outlet blade angle
$\varphi_2$ [°]	486		Wrap angle
Balanced	No	Yes	Dynamic balancing

The solids passage diameter is ensured up to 50 mm by both impellers. The impeller B is dynamically balanced so the center of gravity lies on the rotational axis and the main axis of inertia is identical with the rotational axis.



**Fig. 2.** Impeller A (left) and impeller B (right).

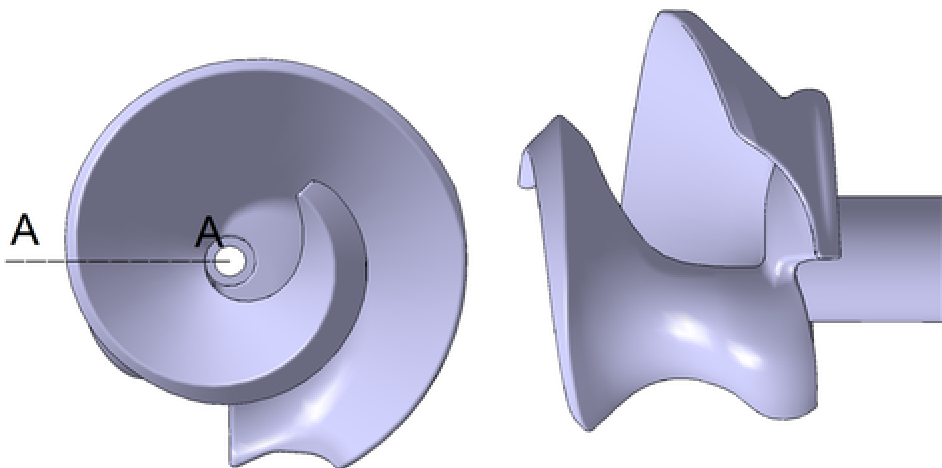


**Fig. 3.** Balancing of the impeller B.

The way of adding a mass on a 3D model of the impeller B in a CAD software is illustrated in the Figure 3. The balancing mass was added so that hydraulic properties and the solids

passage diameter wouldn't get worse. The mass was added in the cut planes passing through the rotational axis – example is the cut A-A indicated in the Figure 3.

### 3 A comparison of properties of the impellers

Hydraulic properties of the impeller A and the impeller B were on the one hand analysed numerically using CFD methods and, on the other hand, experimentally.

CFD simulations were executed with the following solver setup, see also [1]: unstructured mesh, Menter SST turbulence model, steady-state calculation. The mesh was generated by the software ANSYS Meshing. General criteria for the mesh generation were applied in order to achieve a numerical accuracy. Total number of elements of the numerical model of the pump was 19.2 millions (impeller – 15.2 millions; spiral casing – 2.1 millions; suction pipe – 1.9 millions). In the mesh occurred 5.2 millions tetrahedral elements; 13.9 millions three prism elements; and 2.1 million pyramid elements. The calculations were executed in the steady state using frozen rotor method. The impeller was sequentially set up turning into three various positions. The results were subsequently averaged. This approach is accurate enough only close to the optimal point. Therefore, calculation curves are displayed on graphs only in the area close to the optimal point.



**Fig. 4.** A model of the tested pump.

Experiments were carried out on a test rig with a closed water circuit in a laboratory of hydraulic machinery. A body of the tested pump model was made by welding and it's in the Figure 4. An axial gap between the impeller and the stator was considered 0.3 mm during the measurement and CFD simulations. As a transport medium clean water was used during the experiments as well as during the CFD simulations.

Results of calculations and experiments are shown in the form of characteristic curves  $Q-Y$  and  $Q-\eta$  in the Figure 5. Blue curves represent CFD calculations, while red curves are measured experimentally. The Figure 5 shows that adding of the balancing mass didn't influence hydraulic parameters of the pump in the best efficiency point. BEP location  $Q_{opt}$ ,  $Y_{opt}$  and the magnitude of efficiency  $\eta_{opt}$  are differing only negligibly within the measurement uncertainty. Measured curves (blue colour) are differing only at lower flowrates when the impeller B has higher specific energy. Measurement of the impeller B wasn't executed at lower flowrates than 6 l/s. The reason for this is that the radial as well as the axial force acting on impellers is considerable, as shown, for example, the study [5]. According to the fact that the balanced impeller was made from ABS plastic, it might acquire a mechanical destruction of the rotor at lower flowrates.

The fact that the added mass didn't affect hydraulic parameters is confirmed by CFD simulations (red curves). Performance curves  $Q-Y$  of both impellers are identical according to calculations. The problem is a certain difference between calculated and measured curves

Q-Y. This is caused by CFD computational method, which is called “frozen rotor”. This method is not an optimal one for single-blade pumps.

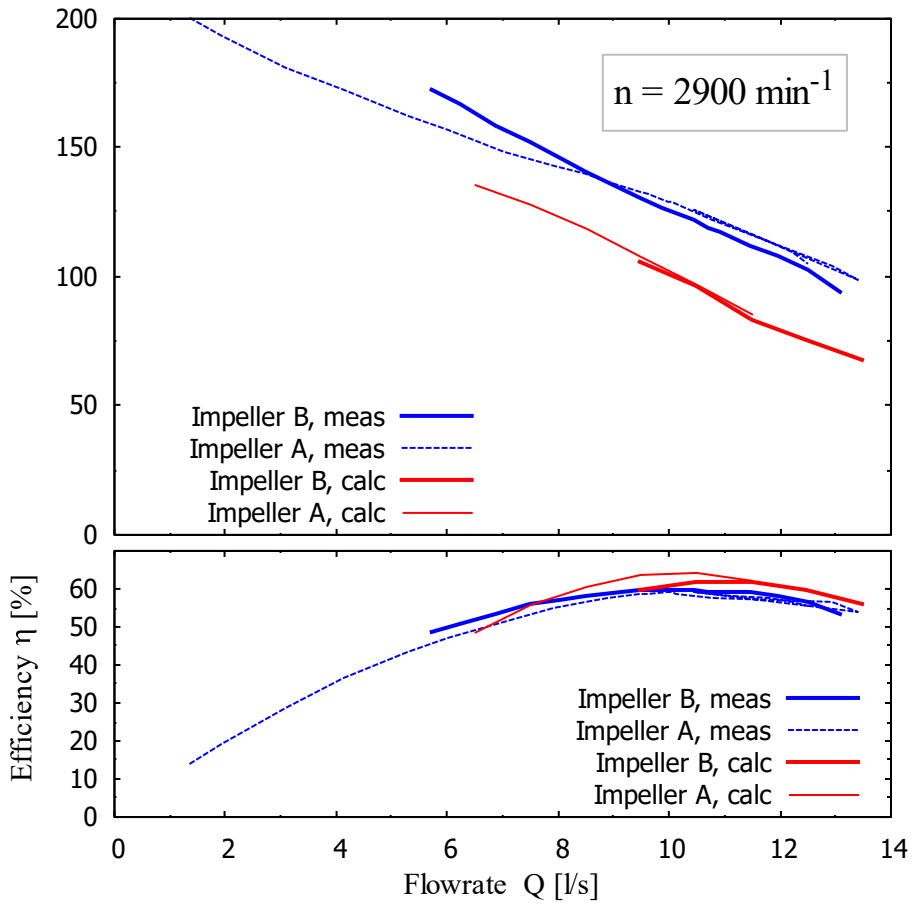


**Fig. 5.** Comparison of measured and calculated data.

**Table 3.** Summary of results – values in BEP.

	Impeller A		Impeller B	
	Meas	Calc	Meas	Calc
$Q_{opt}$ [m <sup>3</sup> /s]	0.010	0.0105	0.0095	0.0105
$Y_{opt}$ [J/kg]	128.6	96.5	130.3	95.8
$\eta_{opt}$ [%]	58.9	64.2	59.5	61.7
Vibrations	YES	-	NO	-

Achieved results are shown in the Table 3. It should be added that the unbalanced impeller A caused vibration of the whole test rig. Despite that, the dynamic balanced impeller B had silent running without vibrations. However, the vibration intensity wasn't measured.

## 4 Conclusions

This paper describes the way of designing the single-blade impeller pump so that mechanical and hydraulic properties requests such as efficiency, BEP location, solids passage diameter and dynamic balancing were fulfilled. The results of the presented research show the following outcomes:

- The shape of blade surface is possible to be designed using basic hydraulic proposal methods, however, it is not possible to ensure dynamic balancing of the impeller. This issue needs to be done additionally, by adding the balancing mass with the help of CAD software. The effect of balancing masses on the flow needs to be monitored by CFD flow simulations.
- It is possible, in case of single-blade pumps, to add the balancing mass so that the total dynamic balancing is achieved and the hydraulic parameters remain unchanged.
- It is possible to achieve high passage diameter unless the balancing mass is added in a position where the flow channel is wide enough.
- CFD methods of flow simulations are giving a relatively good prediction of hydraulic parameters during balancing process of the impeller.

## References

1. B. Knížat, Z. Csuka, M. Hyriak, AIP Conference Proceedings **1768**, 020034 (2016)
2. X. Cheng, R. Li, Procedia Engineering **31**, 914-921 (2012)
3. J.H. Kim, B.M. Cho, Y.S. Kim, Y.S. Choi, K.Y. Kim, J.H. Kim, Y. Cho, International Journal of Fluid Machinery and Systems, Vol. **9**, No. 4, (october-december 2016)
4. H. Quan, R. Li, Q. Su, W. Han, P. Wang, Advances in Mechanical Engineering, Volume **2013** Article ID 512523 (2013)
5. Y. Nishi, J. Fukutomi, R. Fujiwara, IOP Conf. Series: Earth and Environmental Science **15** (2012) 072039
6. Y. Nishi, R. Fujiwara, J. Fukutomi, Journal of Fluid Science and Technology **4** 3 (2009)
7. Y.L. Zhang, Z.C. Zhu, H.S. Dou, B.L. Cui, Y. L. J.J. Xiao Int. J. Turbo Jet-Engines (2015); **32**(1): 59-64